Pattern Analysis & Applications (1998)1:163–177

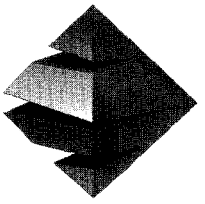

Skeletonisation: An Electrostatic Field-Based Approach[1]

T. Grigorishin, G. Abdel-Hamid[2] and Y.-H. Yang

The Scene Analysis and Modelling Group, Computer Vision and Graphics Laboratory, Department of Computer Science, University of Saskatchewan, Saskatoon, Saskatchewan, Canada

Abstract: Skeleton representation of an object is a powerful shape descriptor that captures both boundary and region information of the object. The skeleton of a shape is a representation composed of idealized thin lines that preserve the connectivity or topology of the original shape. Although the literature contains a large number of skeletonisation algorithms, many open problems remain. In this paper, we present a new skeletonisation approach that relies on the Electrostatic Field Theory (EFT). Many problems associated with existing skeletonisation algorithms are solved using the proposed approach. In particular, connectivity, thinness and other desirable features of a skeleton are guaranteed. It also captures notions of corner detection, multiple scale, thinning, and skeletonisation all within one unified framework. The performance of the proposed EFT-based algorithm is studied extensively. Using the Hausdorf distance measure, the noise sensitivity of the algorithm is compared to two existing skeletonisation techniques. In addition, the experimental results also demonstrate the multiscale property of the proposed approach.

Keywords: Corner detection; Electrostatic-field; Shape analysis; Skeletonisation

1. INTRODUCTION

Shape representation and description plays an important role in most computer vision systems [1]. A useful and reliable shape representation must meet a number of requirements, which include *invariance*, *uniqueness* and *stability* [2,3]. If two objects have the same shape, then their representations should be the same and should be invariant with respect to translation, rotation and scaling. Uniqueness means that if two objects have different shapes they should have different representations. Stability denotes the fact that if two objects have a small shape difference, then their representations should have a small difference. Conversely, if two representations have a small difference, then the objects they represent should also have a small shape difference. Therefore, a stable representation means a representation that is insensitive to noise. In short, the object shape and its representation should have a one-to-one correspondence property.

The representation should reflect the shape of an object at various levels of abstraction and should also combine both boundary and region information of the object. Finally, the shape descriptors and the recognition of objects should be efficiently computable. Other criteria for shape representation can be found in Mokhtarian and Mackworth [3].

The skeleton of a two-dimensional object is a transformation which maps the contour of the object into a set of connected line segments. Skeleton representation as introduced by Blum [4] meets most of the aforementioned requirements.

Since the introduction of the skeleton shape descriptor, many skeletonisation algorithms have been reported in the literature [5]. Many problems, however, remain unsolved. For example, methods to quantitatively evaluate skeletons are still lacking. Recently, some efforts have been made in this direction [6–9].

[1] The authors would like to acknowledge financial support provided by NSERC through grant number OGP0000370.
[2] Gamal Abdel-Hamid passed away on December 4 1994. Grigorishin and Yang would like to dedicate this paper in memory of Abdel-Hamid.
Received: 19 January 1998
Received in revised form: 20 May 1998
Accepted: 23 June 1998

The philosophy of performance analysis, point to the lack of performance evaluation in image analysis algorithms, is also discussed by Haralick [10].

Another problem with most skeletonisation algorithms is their sensitivity to noise. Although there are many skeletonisation algorithms, surprisingly little work has been directed towards studying their sensitivity to boundary noise. Also, some existing skeletonisation approaches require that many parameters be supplied by the user [11].

In this paper, a new skeletonisation approach based on the Electrostatic Field Theory (EFT) for shapes with no holes is proposed. The motivation of this research work stems from the following reasons. First, the encouraging results of a recently developed corner detector based on the same underlying theory, the EFT [12], suggest the possibility of applying the EFT to determine skeletons. Abdel-Hamid and Yang [12] pointed out that electrostatic field lines represent lines of symmetry naturally. Also, EFT presents a natural solution for skeletonisation which can overcome many of the difficulties of existing approaches, such as connectivity and noise sensitivity. Finally, EFT unifies notions of corner detection, thinning, skeletonisation and multiple scale representation of objects, all within the same framework.

This paper is organised as follows. An overview of the related research is discussed in Section 2. The background of the EFT is given in Section 3. The proposed approach for skeletonisation is presented in Section 4. Section 5 describes the performance characterisation experiments and the experimental comparison between the proposed approach, a distance transform based approach [13] and the Charge Particle Method for skeletonisation [14]. Finally, conclusions and future directions are discussed in Section 6.

2. RELATED WORK

This section gives a brief review of skeletonisation algorithms along with their main characteristics and drawbacks. For a more complete survey of skeletonisation algorithms, the interested reader can consult Smith [15].

Existing skeletonisation approaches can be classified approximately into a small number of categories. The first category is based on *topological* or *direct thinning*. Thinning denotes the process of iteratively peeling away the object's contour pixels while preserving its topology [16]. Many thinning techniques have been developed, including both sequential [17] and parallel [18] algorithms. The drawbacks of thinning algorithms are noise sensitivity, loss of continuity and distortion, which usually lead to counter-intuitive results. Most thinning approaches have therefore been directed towards character recognition applications. The reader may refer to Lam et al [16] for a comprehensive survey and bibliography of thinning algorithms.

The second category is to compute the symmetric axes using *direct* or *analytical* methods by approximating the object's boundary by a polygon. For noisy or biological (as cells) objects, this approximation leads to unavoidable inaccuracy. Algorithms belonging to this category are based on either heuristic methods [19–21] or more rigorous methods such as the Voronoi diagram [1,22,23]. Prior to the computation of the Voronoi diagram, the polynomial approximation of the boundary points is computed. Although the Voronoi diagram of n points can be computed in $O(n \log n)$ time in the worst case [24], the proper polynomial approximation of a shape is a difficult task, and becomes essential in the resulting skeletal representation.

The skeletonisation algorithms of the third category are the *ridge following* methods, which are based on a distance transformation applied to the object. A distance transformation converts a binary image into another image where an object's pixels have values corresponding to the minimum distance from the background. Different distance measures can be used, e.g. city-block [25], chessboard [26] and Euclidean [27]. The city-block distance is based on 4-neighbourhood computation, and the chessboard distance is based on 8-neighbourhood computation. Both of these distance measures are linearly additive and are easy to compute. However, the city-block and the chessboard distance measures are sensitive to the rotation of an object, while the Euclidean distance measure is rotation invariant.

After Distance Transformation (DT) the ridges were extracted. By the conventional ridge concept, a ridge is a central elevated surface that rises sharply above two adjacent side surfaces. The projection of these ridges constitutes the skeletal branches of the object. Ridges can be traced by the active contour model [11] and by other methods [28]. For example, the skeletonisation algorithm presented by Smith [15] traces the ridges by choosing the local maxima on the Euclidean (city-block or chessboard) distance transform. The resulting skeleton generated by this method is connected if the object in the original image is connected. However, in the case of several maxima points, different points can be selected, resulting in the possibility of obtaining different skeletonisation results.

The DT-based techniques are relatively simple. In general, the skeletonisation results of this category are more accurate and are smoother than those of the

other two categories [11]. The DT-based algorithms may be run with the option that the resultant skeletal points are labelled with their distance values to the object's boundary. Therefore, the original object can be almost completely recovered by means of a reverse-distance transformation. However, the DT of an object is still sensitive to noise, since the equidistance contours are as noisy as the boundary.

Different DTs have been published in the literature. A comprehensive survey of these approaches is contained in Leymarie and Levine [11]. Some representative examples of this category can be found in Danielsson [29] and Klein and Kubler [27].

A number of algorithms are based on the combination of different features from the aforementioned categories such as the Charge Particle Method (CPM), introduced by Arumugam et al [14]. The CPM considers the object pixels of a binary image as particles with the same charge magnitude and the same charge polarity. The concept of the force of attraction or repulsion between charged particles is used in this algorithm for skeleton generation.

One of the techniques in the DT-based categories is the snake model for computing skeletons [30]. The first step of this approach involves the computation of a specific distance surface, which is equivalent to the Euclidean distance map. The following steps incorporate a physical analogy of the 'grass-fire' method. The snake model provides a natural way of multiscale (dynamic) skeleton representation. By appropriately selecting the scale, the desired level of details of the skeleton can be obtained. However, a limitation of the snake model is that it requires an initialisation process to position the snake close enough to the desired solution.

The EFT-based skeletonisation method has some commonalities with algorithms in the ridge following category, where the DT is replaced by an *electrostatic potential distribution map* and the ridge following process by the tracing of field lines passing through significant convexities and concavities detected along some equipotential contour. The use of the potential distribution in image processing is not new. Current models of the potential distribution calculation are computationally expensive. Recently, an efficient generalised potential field model for shape representation has been developed [31]. The traversal of the skeletal points is performed on the basis of the potential map in the direction of the Newtonian force vector. This model incorporates some features of the CPM and the EFT-based technique. It is, however, applicable only for a two-dimensional polygonal region, and the work lacks in experimental evaluation.

The EFT-based approach for image skeletonisation can represent the object's shape at different levels of smoothing or scale and can capture important shape information such as curvature. Furthermore, equipotential contours are smoother than equidistance contours which are employed in the ridge following category.

3. BACKGROUND OF THE EFT

This section reviews the general concepts of the EFT. For a more detailed description consult Nussbaum [32] or Silvester [33].

1. Let us consider two charged particles separated by a fixed distance R. According to Coulomb's Law, the force acting along the line between two charges can be expressed in the following vector equation:

$$\vec{F} = C\frac{Q_1 Q_2}{R^2}\vec{r}$$

where Q_1 and Q_2 are the magnitude of charges, R is the distance between charges, C is a constant which depends upon the medium, and $\vec{r}$ is a unit vector.

2. The entire region of influence of a charge is called the electrostatic field. Its magnitude is specified by a quantity called the electrostatic field intensity and is denoted by symbol E. The field intensity is defined as the force per unit charge exerted on a given charge in the field, or

$$\vec{E} = \frac{\vec{F}}{Q} = C\frac{Q}{R^2}\vec{r}$$

The corresponding potential distribution may be found as:

$$v = C\frac{Q}{R}$$

3. The electrostatic field intensity vector $\vec{E}(x,y)$ can be computed from the potential $v(x,y)$ as

$$\vec{E} = -\nabla v$$

The following observations can be made: the field is in the direction of the steepest descent of the potential; the field lines are perpendicular contours and are directed from the high to the low potential.

4. The electrostatic field conveys the same information as the curvature of an object boundary, which has been verified both theoretically and experimentally [34]. Electrostatic field extrema along an equipotential contour correspond to curvature extrema: significant convexities and concavities [12]. This property is used while extracting the skeleton of an object.

4. ELECTROSTATIC FIELD-BASED APPROACH TO SKELETONISATION

The various skeletonisation algorithms developed use the binary image of an object as the input. The input to the presented skeletonisation algorithm is a binary image of the boundary of an object. For example, the input to the EFT-based approach can be the edges of the object detected by an edge detector. In the EFT-based method the boundary points are modeled as unit charges, and their values are set to 1 (see Fig. 1).

In the proposed approach, a skeleton is defined as follows: $s = \{(x,y) \mid E(x,y)$ is a local maximum or minimum, or $v(x,y)$ is a maximum potential$\}$ where $v(x,y)$ is the potential at the location (x,y) inside the object, and $E(x,y) = |\nabla v(x,y)|$ is the electrostatic field of the object. S represents the electrostatic field lines passing through points of significant convexities and concavities, and the points of maximum potential. This definition differs from the conventional definition of a skeleton.

The following are the steps required to find the skeleton of a planar object:

1. Compute the potential distribution $V = v(x,y)$ inside the object.
2. Compute the electrostatic field in the x and y directions: E_x and E_y, respectively.
3. Find the equipotential contour at a given potential v_{con}.
4. Detect significant convexities and concavities along an equipotential contour.
5. Trace skeletal points starting from points of significant convexities and concavities.

The following sections give details of each of the above steps.

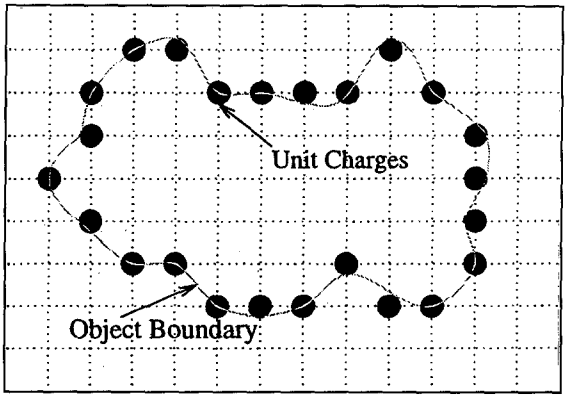

Fig. 1. The image model to generate the potential distribution of the object boundary.

4.1. Solution of the Potential Distribution Inside the Object

The method presented of computation of the potential distribution inside the object uses a predefined structuring element. The structuring element M is as large as the image. The value of the element at location (x,y) is $\frac{1}{\sqrt{(x^2+y^2)}}$. It gives the contribution of a unit charge located at that location because the electrostatic potential $v(x,y)$ at the centre is inversely proportional to the distance between (x,y) and the centre of the mask. Hence, the total potential at the centre of the mask is the summation of all the potentials due to charges within the neighbourhood of the mask. The potential distribution is given by the convolution of M with the input image, which can be computed efficiently using the Fast Fourier Transform (FFT). The FFT of M is computed and is then pointwise multiplied with the FFT of the input image. The inverse FFT is then performed to obtain the potential field distribution of the image.

After the potential distribution is computed, it is normalised as follows. The potentials outside the object boundaries are set equal to 0. The maximum potential is set equal to 255. The potential values inside the object are then normalised using a simple linear transformation.

4.2. Solution of the Electrostatic Field of the Object

The proposed approach for skeleton tracing uses the electrostatic field computed in the x and y directions: E_x, and E_y, respectively. The computation for E_x and E_y uses two structuring elements, M_x and M_y, for the x and y directions, respectively. Each entry of the x-direction mask M_x is computed as $-x/r^3$, where r is the distance from the centre of the mask. A similar operation is used to compute the y-direction mask M_y. The electrostatic fields, E_x and E_y, are given by the convolution of the image with M_x and M_y, respectively, using the FFT, similar to that for the computation of the potential distribution.

4.3. Construction of an Equipotential Contour at a Given Potential

The equipotential contour is used to detect significant convexities and concavities along the contour from which skeletal branches are initiated. This step can be visualised as a potential surface $V = v(x,y)$ being cut by a constant potential plane (parallel to the $x-y$

plane). The curve that results from the intersection of the potential surface and the cutting plane is a closed contour.

The construction of a connected equipotential contour at a user specified potential v_{con} within the range 0–255, is based on the E_x and E_y maps, and is described as follows.

First, based on the potential map, the starting point (x_0,y_0) at which the potential is equal to v_{con} is detected. Starting from this point, the equipotential contour is built at subpixel resolution. It is well known that the equipotential contour is perpendicular to the field lines. Therefore, the tracing direction of the contour is perpendicular to that given by the direction of the electrostatic field, which is specified by $E_x(x,y)$ and $E_y(x,y)$. Suppose that the present location is at (x_{n-1},y_{n-1}). The next point (x_n,y_n) of the equipotential contour is determined as follows:

$$x_n = x_{n-1} - E_y(x_{n-1},y_{n-1}) \times \delta$$
$$y_n = y_{n-1} + E_x(x_{n-1},y_{n-1}) \times \delta$$

where δ is the step size. δ determines the accuracy of the computation of the potential contour at the subpixel level. A larger value of δ (e.g. up to 10) will result in faster computation of the potential contour. However, it might result in larger accumulation error and the curve might not necessarily close itself, in which case additional checks are performed to connect the last point of the equipotential contour with the first one. In the implementation, δ is chosen to be 1 for all experiments. The result of this step is a curve $E(s)$ at the given potential v_{con}.

It is worth noting that the larger the value of the contour potential v_{con}, the smoother is the contour, the less the number of extrema of the field, and the less the number of significant convexities and concavities. This is expected due to the smoothing effect of the solution of the potential distribution inside the object.

From the above discussion, it is evident that the proposed skeletonisation approach has the advantage of a multiscale approach. By appropriately choosing the equipotential contour at potential v_{con}, the desired level of details (or scale) of the skeleton can be selected. In particular, choosing an equipotential with a high value of v_{con}, a coarse skeleton is generated, whereas choosing an equipotential with a low value of v_{con}, a fine skeleton is generated. Such a smoothing effect has been used previously in reconstructing the three-dimensional default shape of an object from its occluding contour. Figure 2 shows this interesting property of the potential distribution by depicting some equipotential contours of the maple leaf at various potentials.

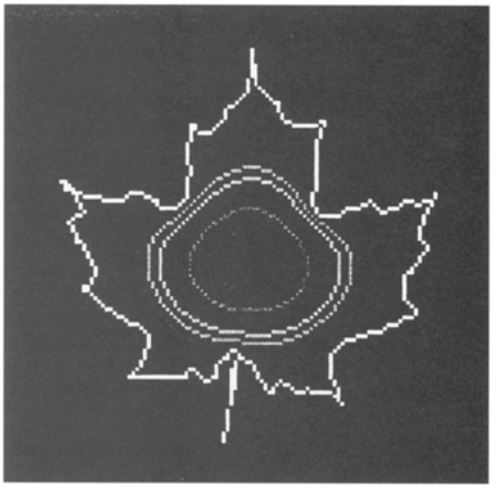

Fig. 2. Smoothing effect and multiscale property of equipotential contours of the maple leaf. The white contour is the boundary. The grey contours are the equipotential contours. The equipotential contours shown are constructed in the potential range 0–255 in steps of 10. When the contour is closer to the centre of the object, the contour gets smoother and details tend to disappear.

4.4. Detecting Corners along the Equipotential Contour

Starting from the field distribution $E(s)$ along the contour s, convex (concave) corners are located by identifying points having local minima (maxima) of the field $E(s)$. As mentioned in the previous step, the choice of the contour potential v_{con} directly determines the degree of detail of the skeleton. Figure 3 demon-

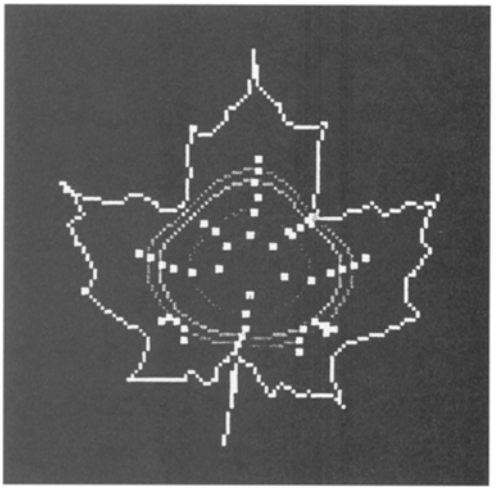

Fig. 3. The equipotential contours and their associated corners (bright dots) of the maple leaf. The contours are constructed for the potential range 0–255 in steps of 10. The white contour is the boundary. As the potential v_{con} decreases, the number of corners decreases.

strates this fact by depicting different equipotential contours and their associated detected corners. The lower is the potential, the lower the number of corners detected. Corners merging, disappearing, attracting and repelling can also be seen in the figure.

In this paper, both convex and concave corners are employed in generating skeletal branches. Corners are detected using the approach as described by Abdel-Hamid and Yang [12]. Many skeletonisation algorithms consider only convex corners (e.g. [17]). Considering only convexities may be justified in certain applications, as in the identification of pseudopods [17], but both convexities and concavities must be considered because both contribute equally to the shape of an object. For a unique skeleton representation, both convexities and concavities must be considered (see Fig. 4).

4.5. Skeleton Tracing

Having identified points of significant convexities and concavities along an equipotential contour at potential v_{con}, these points are used to initiate the skeleton tracing procedure. The skeleton branches correspond to field lines passing through significant corners identified in the previous step. Therefore, the skeleton generation procedure is reduced to the problem of tracing the field lines.

Starting from the points having significant convexities and concavities along an equipotential contour of potential v_{con}, the field lines are traced in two directions: in the inward direction (uphill generation) towards the object's central region or pixel; and in the outward direction (downhill generation) towards the object's boundary. Tracing is done in the direction defined by $E_x(x,y)$, $E_y(x,y)$.

When tracing downhill toward the object's boundary, the location of the next point (x_n,y_n) is defined at subpixel resolution as follows:

$$x_n = x_{n-1} - E_x(x_{n-1},y_{n-1}) \times \delta$$

$$y_n = y_{n-1} - E_y(x_{n-1},y_{n-1}) \times \delta$$

As before, δ is chosen to be 1. This process terminates when the object's boundary is reached, i.e. at the global minimum potential.

The same process is used for the uphill generation towards the central region of the object. The next point is defined at subpixel resolution as follows:

$$x_n = x_{n-1} + E_x(x_{n-1},y_{n-1}) \times \delta$$

$$y_n = y_{n-1} + E_y(x_{n-1},y_{n-1}) \times \delta$$

This process terminates at the object's central pixel or region, i.e. at the maximum potential.

It is noteworthy that the skeletal branches generated by this procedure are guaranteed to meet at the maximum potential region, since the potential distribution increases monotonically in the inward direction up to the maximum potential. Also, the connectivity requirement of the skeleton is guaranteed using this approach, because the electrostatic field lines must be continuous [35].

5. EXPERIMENTAL RESULTS AND ANALYSIS

The main objective of any thinning algorithm is to obtain a connected skeleton of unit width along the medial axis of a given pattern. The resulting skeleton should inherit all the topological features of the original image. The following characteristics are usually used to judge the quality of the resulting skeletons: connectivity, thinness, symmetry of the skeleton and sensitivity to noise. Computational complexity of the skeletonisation algorithm and its reconstruction abilities are also important characteristics considered in the literature.

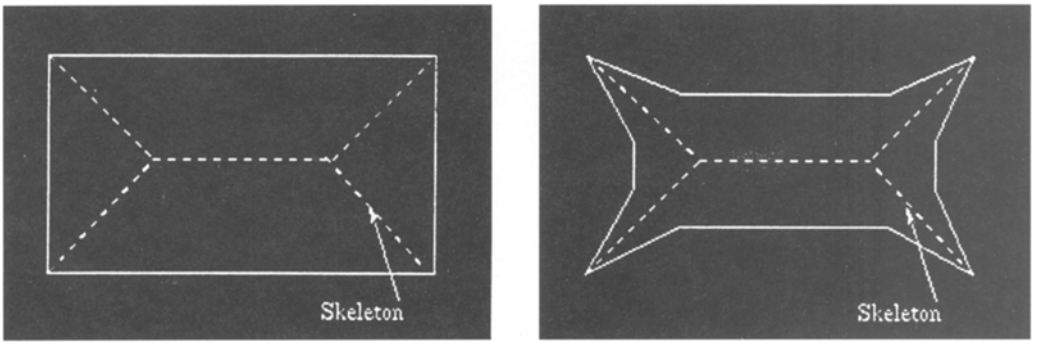

Fig. 4. The same skeleton for different shapes. Considering only convexities and disregarding concavities leads to non-unique skeleton representation.

A number of experiments were conducted using both synthesised and real images on a DEC AlphaServer Model 2100 with 256 MB of memory, running OSF/1 V3.0.

We present the experimental results obtained by the EFT-based approach, a skeletonisation algorithm based on the Euclidean Distance Transform [36] and the Charge Particle Method [14]. The EFT-based, DT-based and CPM algorithms are written in the C programming language. Tools in the Cantata visual programming environments were also employed [37]. Arumugam et al [14] pointed out that the CPM is almost as fast as the DT-based approach. The proposed method also has the same order magnitude in performance as the other two methods. A more quantitative timing analysis is beyond the focus of this paper. Figure 5 illustrates skeletons generated for a noise-free image using these techniques.

The proposed algorithm may be run with the option that the resultant skeleton points are labelled with their distance values to the object's boundary. Therefore, the original object can almost completely be recovered by means of a reverse-distance transformation. The Euclidean distance values are computed only for the skeletal points. The Charge Particle Method and DT-based algorithm that are used in this paper also allow reconstruction of the original pattern, for example, by adopting the approach described by Pavlidis [38].

The connectivity and thinness requirements of the skeleton generated by the proposed approach are guaranteed, as explained above. Other thinning techniques do not always satisfy these requirements. The morphological thinning algorithm [39] does not give connected skeletons.

To test the noise sensitivity, the boundary of the object is perturbed in the x and y directions by varying degrees of zero-mean Gaussian noise. The standard deviation σ of the noise is varied in the range from 0 to 20.

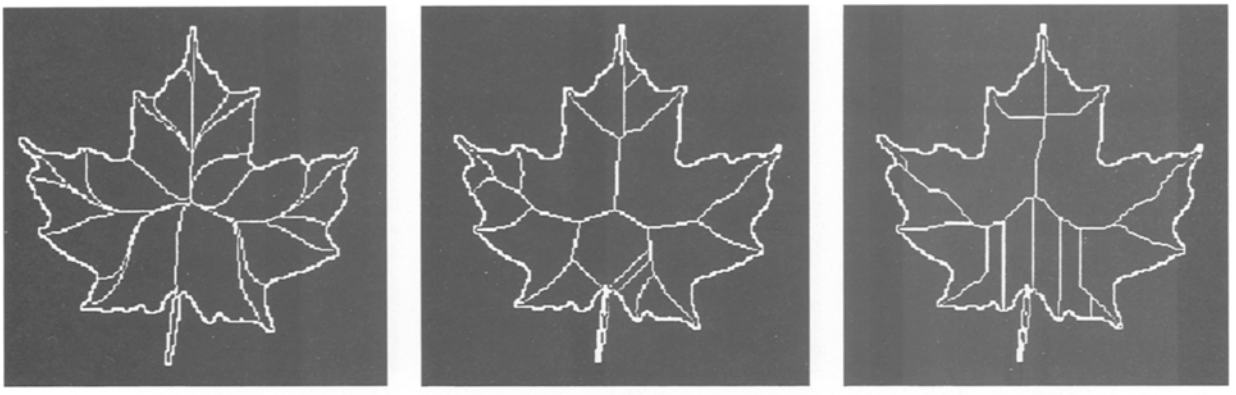

Fig. 5. Skeletons generated for the image of a maple leaf. (a) EFT-based approach. Skeleton started at the equipotential contour 175; (b) DT-based algorithm; (c) Charge Particle Method.

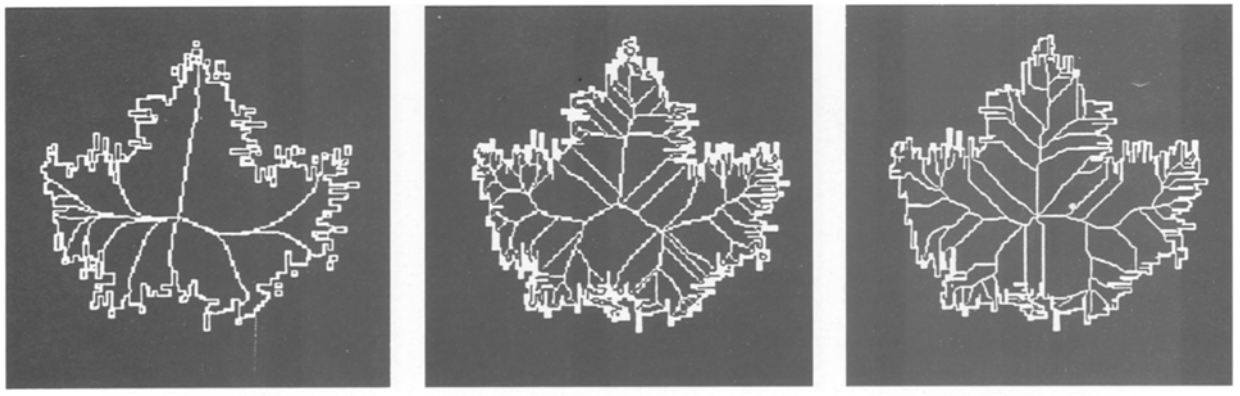

Fig. 6. Skeletons generated for the image of a maple leaf with boundary corrupted with noise of $\sigma = 4$. (a) EFT-based approach. Skeleton started at the equipotential contour 175; (b) DT-based algorithm; (c) Charge Particle Method.

Figure 6 shows the results of skeletonisation for the maple leaf image with boundary corrupted with noise of $\sigma = 4$. Figure 7 illustrates the results for $\sigma = 10$ noise level. One can clearly see that the skeleton generated by the EFT-based approach is insensitive to the presence of boundary noise, whereas the skeletons generated by both the Euclidean distance algorithm and the Charge Particle Method are very sensitive to the presence of boundary noise.

The experimental results for the image of a rectangle are demonstrated in Figs 8 and 9. The boundary of the original image is corrupted with noise of $\sigma = 4$. Analysing the results presented, one can see that the EFT-based method is less sensitive to boundary noise than both the Euclidean DT-based method and the Charge Particle Method.

The Charge Particle Method for the noise-free image of a rectangle produces a different skeleton than expected. This can be explained by the nature of the CPM. The CPM models the object pixels of a binary image as charged particles. It assumes that the boundary of the object is maintained under higher potential than the particles. Therefore, the movement of the particles towards the medial axis is accomplished by the interaction of the electrostatic forces between individual particles and the entire boundary. In each pass, the CPM deletes a set of edge points from the input. Each edge point is tested against the conditions for its removal. The process is repeated iteratively until all the particles attain a state of equilibrium when the resulting force acting on them is zero. For objects such as rectangles and ellipses, all the conditions of the CPM for particle removal are satisfied, because the CPM assumes that the resultant force acting on a certain particle is due to the cumulative effect of eight immediate neighbouring particles. This restriction was proposed based on the observation that the force acting between particles is inversely proportional to

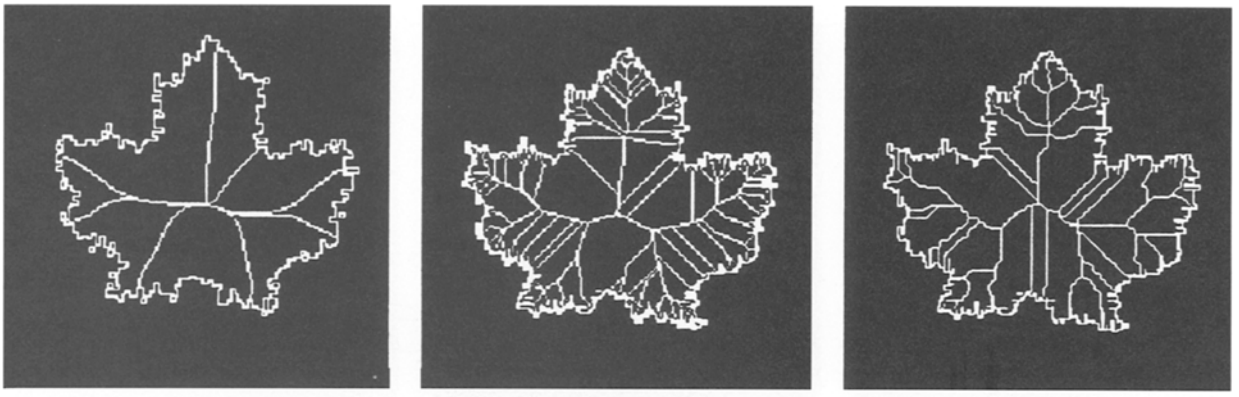

Fig. 7. Skeletons generated for the image of a maple leaf with boundary corrupted with noise of $\sigma = 10$. (a) EFT-based approach. Skeleton started at the equipotential contour 175; (b) DT-based algorithm; (c) Charge Particle Method.

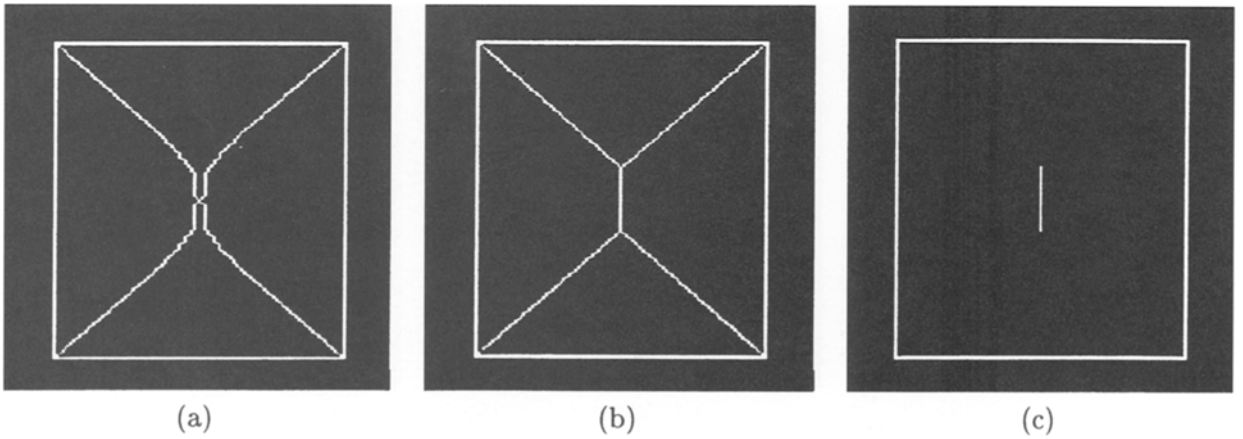

Fig. 8. Skeletons generated from the image of a rectangle. (a) EFT-based approach. Skeleton started at equipotential contour 75; (b) DT-based method; (c) Charge Particle Method.

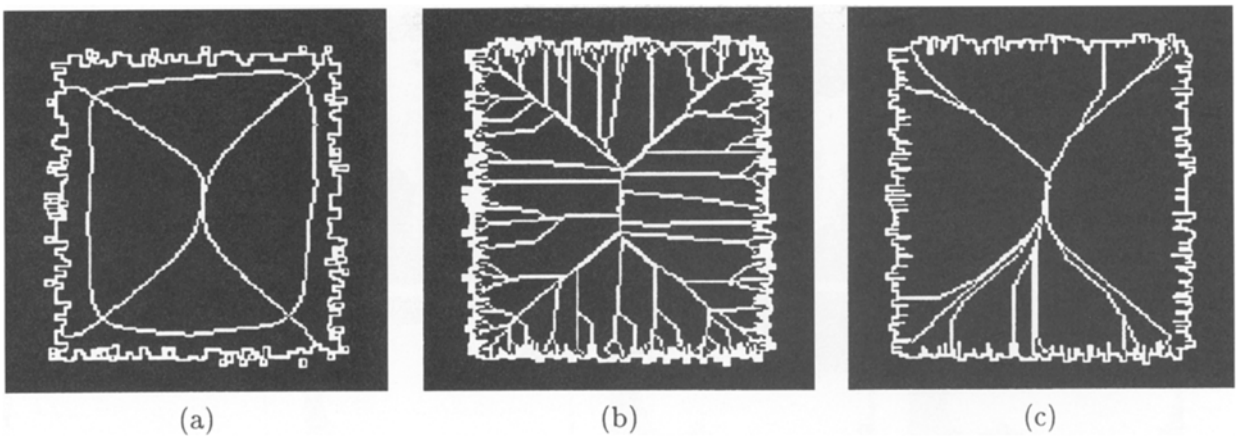

Fig. 9. Skeletons generated from the image of a rectangle with boundary corrupted with a noise of $\sigma = 4$. (a) EFT-based approach. Skeleton started at equipotential contour 115; (b) DT-based algorithm; (c) Charge Particle Method.

the square of the distance between them [14]. At each iteration, all edge points for such a type of image are removed, resulting in incorrect thinning of the pattern.

We compare the performance of the proposed skeletonisation approach with the DT-based algorithm and the CPM in the presence of noise using the Hausdorf distance measure [9,40]. Given two sets A and B, the Hausdorf distance is defined by $H(A,B) = \max \{\min \{r \mid A \subseteq B \oplus disk(r)\}, \min \{r \mid B \subseteq A \oplus disk(r)\}\}$, where $\oplus$ is the standard sum notation. $H(A,B)$ measures the degree of match between the two sets, A and B, by computing the furthest distance of A from B.

For each algorithm, in this experiment, the image of the rectangle was used. The image size is 256×256. The skeleton generated for a noise-free image is compared to that generated for images at different levels of boundary noise that varies in the range from 2 to 20. Figure 10 shows the variation of the Hausdorf distance measure versus the level of noise present in the input image for the skeletonisation. As can be seen in Fig. 10, the EFT-based approach is less sensitive to noise as compared with the DT-based approach and the Charge Particle Method.

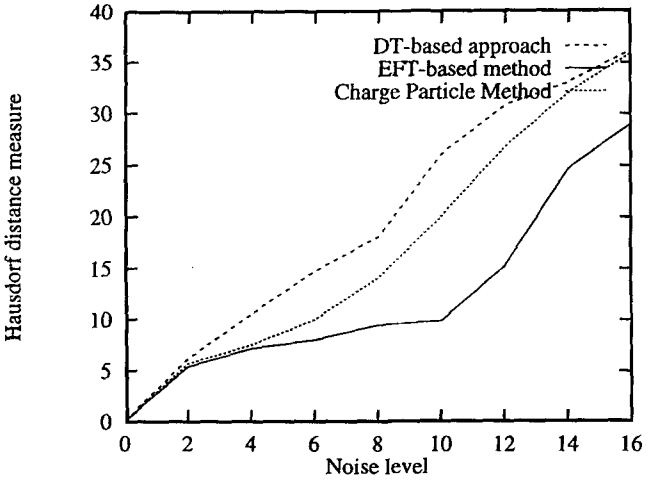

Fig. 10. The Hausdorf distance measure between the skeleton for a noise-free image and the skeletons for the images with different levels of boundary noise.

We have seen the experimental results of skeletons of a rectangle with boundary corrupted with various noise level (Figs 8 and 9). It can be seen that the skeletons extracted by the proposed approach is quite insensitive to boundary noise. This is due to the smoothing effect of the potential field. However, the Hausdorf distance does not fully reflect this fact. The maple leaf image was not employed in this experiment because the number of branches in the skeletons varies with the noise level. As a result, the Hausdorf distance measure is very high, and does not appear to reflect the quality of the extracted skeletons.

The objective of the next two experiments is to further study the effect of a different type boundary noise, namely greyscale noise, as well as the multiscale property of the proposed EFT-based skeletonisation algorithm. It is noteworthy that the proposed approach does not require the boundary of the object to be detected, while existing skeletonisation techniques do. In the case of a greyscale image, the input to the proposed approach is obtained by mapping the grey level of the input image to the charge value. The following images are used for the experiments:

1. Binary images are synthesised from a tree generated by a simple L-system. The number of generations is specified by the user. At each pixel in the tree, a circle of random radius is added to the image. Some of the images synthesised by this method are illustrated in Fig. 11a. Noisy images are generated by adding to the image 0-mean grey level Gaussian boundary noise with σ ranging from 0 to 20 in steps of 4 (see Figs 11b–d).

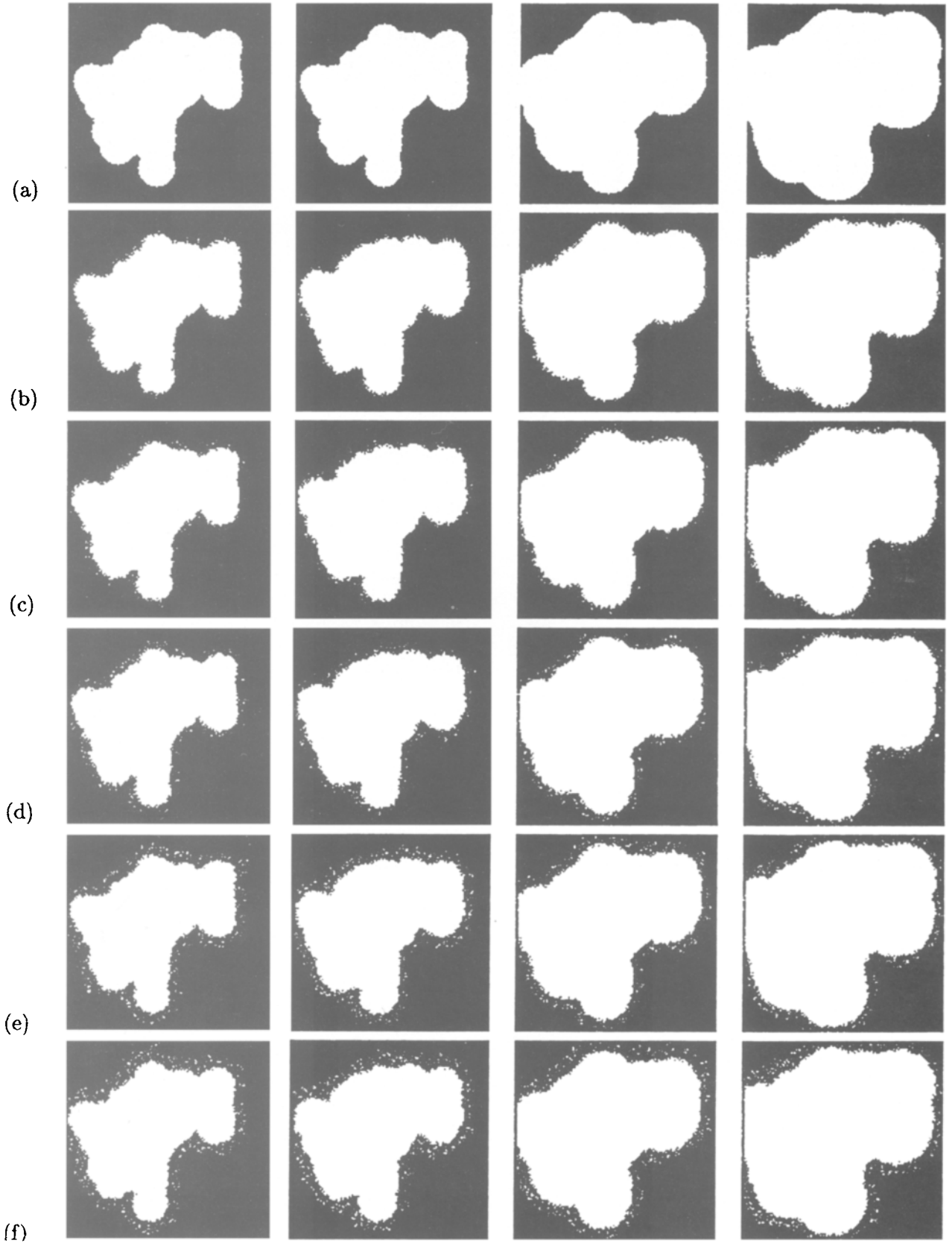

Fig. 11. Binary images for image skeletonisation with boundary corrupted with 0-mean Gaussian noise of: (a) $\sigma = 0$ (noise free); (b) $\sigma = 4$; (c) $\sigma = 8$; (d) $\sigma = 12$; (e) $\sigma = 16$; (f) $\sigma = 20$.

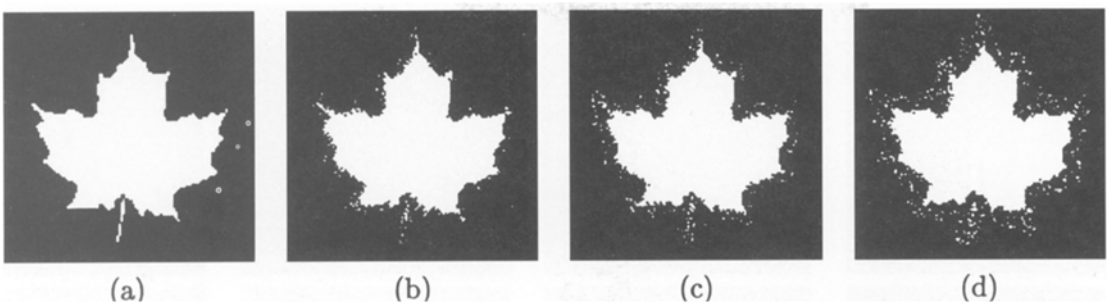

Fig. 12. Real images for image skeletonisation with boundary corrupted with 0-mean Gaussian noise of: (a) $\sigma = 0$ (noise free); (b) $\sigma = 8$; (c) $\sigma = 12$; (d) $\sigma = 20$.

2. Real images (see Fig. 12a). Noisy images are generated similarly (see Figs 12b–d).

The results of the EFT-based skeletonisation of binary images are illustrated in Fig. 13. It can be seen that the extracted skeletons are insensitive to boundary noise.

The EFT-based skeletonisation method allows the representation of the skeleton across a variety of scales. These multiscale skeletal representations can be obtained by changing the starting potential value for skeleton generation. At a finer scale (smaller starting potential value), the skeleton has a large number of branches. At a coarser scale (larger starting potential value), the skeleton has fewer branches and is less sensitive to noise. Figure 14 clearly demonstrates this multiscale capability of the EFT-based approach. The skeletons generated at a potential of 200 (Fig. 14a) are finer in scale, and hence have a larger number of branches when compared to those generated at a potential of 250 (Fig. 14e).

6. CONCLUSIONS AND FUTURE WORK

In this paper, a new approach for skeletonisation that relies on the EFT has been presented. The details of the steps that constitute the proposed skeletonisation approach have been described. The approach has been shown to possess a number of desirable features that can naturally solve many problems that have challenged existing skeletonisation approaches. First, the connectivity and thinness properties are guaranteed in the proposed approach. Secondly, the EFT approach gracefully captures and unifies notions of corner detection, multiscale representation, thinning and skeletonisation. Thirdly, the insensitivity of the proposed approach to severe boundary noise has been demonstrated experimentally. Moreover, since the new skeletonisation approach is developed based on a well-established theory, the electrostatic field theory, the performance of the proposed approach under varying conditions can be predicted and justified before experiments are even conducted.

The potential distribution in its own constitutes a useful representation of objects at various levels of detail, similar to the multiscale curvature-based shape representation approach [2,3]. In the proposed approach, a skeleton of a given scale corresponds to the skeleton generated using a given potential. Consequently, the potential map captures all the skeletons of all scales. In fact, the equipotential contours generated from the potential surface can be viewed as fingerprints of the object [41] for robust representation and recognition, the application of which is an interesting research topic.

Experimentally, we found that the Hausdorf distance measure does not fully reflect the experimental results obtained. Thus, the evaluation of skeletons is still an open issue.

The extension of EFT-based approach for shapes with holes is beyond the study of this paper. To extend this model to work for images with holes, we can model the boundaries of the object with different potential values, e.g. positive charges to the outer boundary and negative charges to the boundaries of holes.

Our research work using the EFT framework for solving computer vision problems inspires further research using the same approach in addressing other vision problems. A natural extension to the EFT-based approach is to use it in representing multidimensional objects. The potential surface becomes the *potential volume* and the equipotential contours are replaced by equipotential surfaces. Also, the electrostatic field extrema would correspond to curvature extrema, and hence three-dimensional edges and corners can be detected using the same methodology described in this paper. Once the potential volume is estimated, the three-dimensional skeleton of a three-dimensional

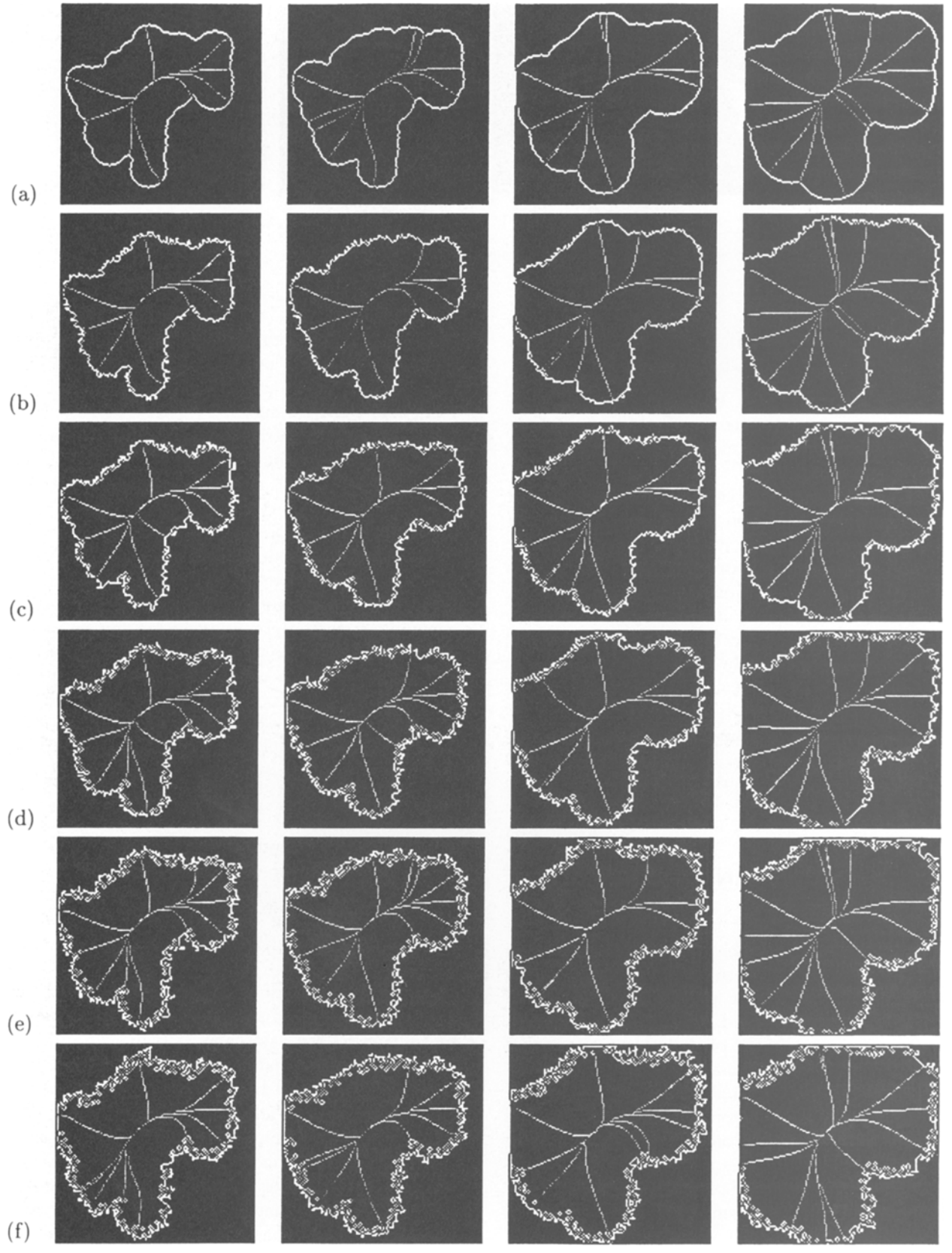

Fig. 13. EFT-based skeletonisation results for the binary images depicted in Fig. 11. $V_{con} = 220$. The white contour is the boundary. The boundary of the images is corrupted with a noise of: (a) $\sigma = 0$ (noise free); (b) $\sigma = 4$; (c) $\sigma = 8$; (d) $\sigma = 12$; (e) $\sigma = 16$; (f) $\sigma = 20$.

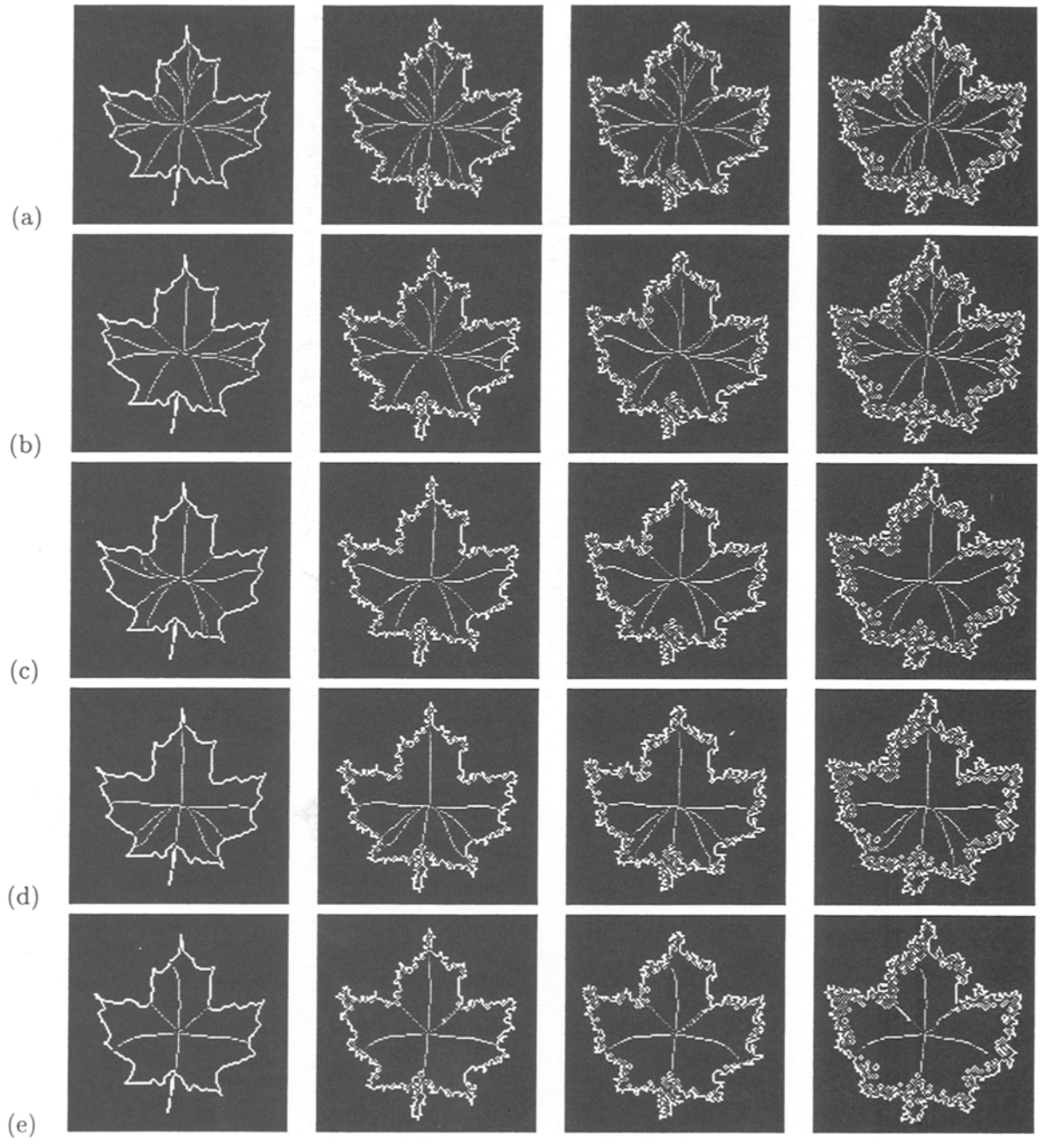

Fig. 14. The multiscale capability of the EFT-based skeletonisation approach. Skeletons generated: the images depicted in Fig. 12. The white contour is the boundary. (a) $v_{con} = 210$; (b) $v_{con} = 220$; (c) $v_{con} = 230$; (d) $v_{con} = 240$; (e) $v_{con} = 250$.

object [28,42], which has a special importance in biomedical applications, can be extracted. Recent extensions to the proposed approach include applications of the EFT approach to segmentation [43] and form segmentation [44].

The experience in this work suggests that interesting features exhibited by the electrostatic field-based approach of corner detection and skeletonisation promote the investigation of more physics-based models in solving computer vision problems. Finally, it is

believed that borrowing simple ideas from other disciplines, such as physics, will certainly benefit research in the computer vision community.

References

1. Maya N, Rajan VT. An efficient shape representation scheme using Voronoi skeletons. Pattern Recognition Letters 1995; 16: 147–160
2. Mokhtarian F, Mackworth AK. Scale-based description and recognition of planar curves and two-dimensional shapes. IEEE Transactions on Pattern Analysis and Machine Intelligence 1986; 8(1): 34–43
3. Mokhtarian F, Mackworth AK. A theory of multiscale, curvature-based shape representation for planar curves. IEEE Transactions on Pattern Analysis and Machine Intelligence 1992; 14(8): 789–805
4. Blum H. A transformation for extracting new descriptors of shape. In Models for the Perception of Speech and Visual Form, Wathen-Dunn W. (ed). MIT Press, 1967
5. Vega OE, Yang YH. Default shape theory: with application to the computation of the direction of the light source. CVGIP: Image Understanding 1994; 60(3): 285–299
6. Lam L, Suen CY. Automatic evaluation of skeleton shapes. Proceedings 11th International Conference on Pattern Recognition, The Hague, The Netherlands 1992; 342–345
7. Lee SW, Lam L, Suen CY. Performance evaluation of skeletonization algorithms for document image processing. Proceedings 1st International Conference on Document Analysis and Recognition, St. Malo, France 1991; 260–271
8. Plamondon R, Suen CY. On the definition of reference skeletons for comparing thinning algorithms. Proceedings Vision Interface 1988, Edmonton, Canada, 1988; 70–75
9. Jaisimha MY, Haralick RM. A methodology for the characterization of the performance of thinning algorithms. Proceedings 2nd International Conference on Document Analysis and Recognition, Tsukuba, Japan 1993; 282–286
10. Haralick RM. Performance characterization in image analysis: thinning, a case in point. Pattern Recognition Letter 1992; 13: 5–12
11. Leymarie F, Levine MD. Simulating the grassfire transform using an active contour model. IEEE Transactions on Pattern Analysis and Machine Intelligence 1992; 14(1): 56–75
12. Abdel-Hamid, GH, Yang, YH. Electrostatic field-based detection of corners of planar curves. Proceedings of the 1993 Canadian Conference on Electrical and Computer Engineering, Vancouver, Canada 1993; 767–770
13. Shin FY, Mitchell OR. A mathematical morphology approach to Euclidean distance transformation. IEEE Transactions on Image Processing 1992; 1(2): 197–204
14. Arumugam A, Radhakrishnan T, Suen CY. A thinning algorithm based on the force between charged particles. International Journal of Pattern Recognition and Artificial Intelligence 1993; 7(5): 988–1008
15. Smith RW. Computer processing of line images: A survey. Pattern Recognition 1987; 20(1): 7–15
16. Lam L, Lee SW, Suen CY. Thinning methodologies – a comprehensive survey. IEEE Transactions on Pattern Analysis and Machine Intelligence 1992; 14(9): 869–885
17. Dill AR, Levine MD, Noble PB. Multiple resolution skeletons. IEEE Transactions on Pattern Analysis and Machine Intelligence 1987; 9: 495–504
18. Guo Z, Hall RW. Fast fully parallel thinning algorithms. CVGIP: Image Understanding 1992; 55(3): 317–328
19. Arcelli C. Pattern thinning by contour tracing. Computer Graphics Image Processing 1981; 17: 130–144
20. Martinez-Perez MP, Jimenez J, Navalon JL. A thinning algorithm based on contours. Computer Graphics and Image Processing 1987; 39: 186–201
21. Shapiro B, Pisa J, Sklansky J. Skeleton generation from x, y boundary sequences. Computer Graphics and Image Processing 1981; 15: 136–153
22. Brandt JW, Algazi VR. Continuous skeleton computation by Voronoi diagram. CVGIP: Image Understanding 1992; 55(3): 329–338
23. Ogniewicz R, Ilg M. Voronoi skeletons: theory and applications. Proceedings IEEE Conference on Computer Vision and Pattern Recognition, Champaign, IL, 1992; 63–69
24. Aurenhammer F. Voronoi diagrams: A survey of a fundamental geometric data. ACM Computing Surveys 1991; 23: 345–504
25. Arcelli C, Sanniti di Baja G. A one-pass two-operations process to detect the skeletal pixels on the 4-distance transform. IEEE Transactions on Pattern Analysis and Machine Intelligence 1989; 4: 411–414
26. Arcelli C, Sanniti di Baja G. A width independent fast thinning algorithm. IEEE Transactions on Pattern Analysis and Machine Intelligence 1985; 7: 463–474
27. Klein F, Kubler O. Euclidean distance transformation and model guided image interpretation. Pattern Recognition Letters 1987; 3: 19–30
28. Gauch J, Pizer S. The intensity axis of symmetry and its application to image segmentation. IEEE Transactions on Pattern Analysis and Machine Intelligence 1992; 15(8): 753–770
29. Danielsson PE. Euclidean distance mapping. Computer Graphics and Image Processing 1980; 14: 227–248
30. Leymarie F. Tracking and describing deformable objects using active contour models. MSc thesis, McGill University, Montreal, Quebec, Canada, 1990
31. Ahuja N, Chuang JH. Shape representation using a generalized potential field model. IEEE Transactions on Pattern Analysis and Machine Intelligence 1997; 19: 169–176
32. Nussbaum A. Field Theory. Charles E. Merrill Books, 1967
33. Silvester P. Modern Electromagnetic Fields. Prentice-Hall, 1967
34. Mittra R, Lee SW. Analytical Techniques in The Theory of Guided Waves. McMillan, 1971; 4–11
35. Fuller AJB. Engineering Field Theory. Pergamon Press, 1973
36. Shin FY, Pu CC. A skeletonization algorithm by maxima tracking on Euclidean distance transform. Pattern Recognition 1995; 28(3): 331–341
37. Khoros, Krohos Research Inc., 1994
38. Pavlidis T. An asynchronous thinning algorithm. Computer Graphics and Image Processing 1982; 20: 133–157
39. Giardina CR, Dougherty E. Morphological Methods in Image and Signal Processing. Prentice-Hall, 1988
40. Haralick RM, Shapiro LG. Computer and Robot Vision. Addison-Wesley, 1992
41. Piech MA. Comment on fingerprints of two-dimensional edge models. Computer Vision, Graphics and Image Processing 1988; 42: 381–386
42. Nguyen T, Sklansky J. Reconstructing the 3-D medical axes of coronary arteries in single-view cineangiograms. IEEE Transactions on Medical Imaging 1994; 13(1): 61–73
43. Grigorishin T, Yang YH. Image segmentation: An electrostatic field based approach. Vision Interface 98, Vancouver, BC, June 18–20 1998
44. Grigorishin T, Yang YH. Form segmentation: An electrostatic field based approach. Technical Report, Department of Computer Sciences, University of Saskatchewan, 1997

Tanya Grigorishin received her MSc in Computer Science in 1997 from the University of Saskatchewan, Saskatoon, SK. Her BSc is in Applied Mathematics from the Chernivtsi State University, Chernivtsi, Ukraine. Tanya is currently working at Hampson-Russell Software Services in Calgary as an application programmer.

Yee-Hong Yang received a BSc degree (with first class honours) in physics from the University of Hong Kong, MS degree in physics from Simon Fraser University in Canada, MSEE and PhD degrees in electrical engineering from the University of Pittsburgh. From 1980 to 1983, Dr Yang was a research scientist in the Computer Engineering Center of Mellon Institute, a division of Carnegie-Mellon University, where he was involved in the Very High Speed Integrated Circuit (VHSIC) program. In 1983, he joined the Department of Computational Science (now called the Department of Computer Science) at the University of Saskatchewan, and currently holds the rank of full professorship and is the founding Director of the Computer Vision and Graphics Lab. From July 1 1989 to June 30 1990, he spent his sabbatical at the McGill Research Center for Intelligent Machines of McGill University in Montréal, Québéc, Canada. Since July 1 1996, he has collaborated with Alias | Wavefront on projects related to both computer vision and computer graphics. Dr Yang's research interests include image processing, computer vision, motion analysis, biomedical image processing and computer graphics, in particular, animation. He is a senior member of the IEEE, and is a member of the ACM, the Pattern Recognition Society and the Optical Society of America. In addition to his refereeing activities, he serves on the Editorial Board of *Pattern Recognition*. In 1998, he serves as program co-chair of Vision Interface 98.

Correspondence and offprint requests to: Y-H Yang, Department of Computer Science, University of Saskatchewan, Saskatoon, Saskatchewan, Canada S7N 5A9. Email: yang@cs.usask.ca.